

ガンマ線偏光計HARPOの試験

所属	Ecole Polytechnique LLR	ビームライン	BL01
利用者氏名	Denis Bernard	利用分野	量子ビーム技術
利用年度	2015年度	活用技術	ガンマ線利用

利用成果の概要

The HARPO time projection chamber (TPC) was installed in a polarised gamma-ray beamline at NewSUBARU. This is a high angular resolution telescope for gamma-ray polarimetry. Data were taken at photon energies from 1.7 MeV to 74 MeV, and with different polarisation configurations. The experimental setup of the TPC and the photon beam are described attached figures. The first results from the beam campaign are shown in attached papers.

HARPO時間投影チェンバー (Time Projection Chamber)をNewSUBARU偏光ガンマ線ビームラインに設置した。これはガンマ線偏光測定のための高角度分解望遠鏡である。

光子エネルギー1.7MeVから74MeVで異なる偏光条件で、データの取得を行った。ガンマ線ビームとTPCの実験配置を図に示す。実験結果の最初の形跡結果を、添付論文に示す。

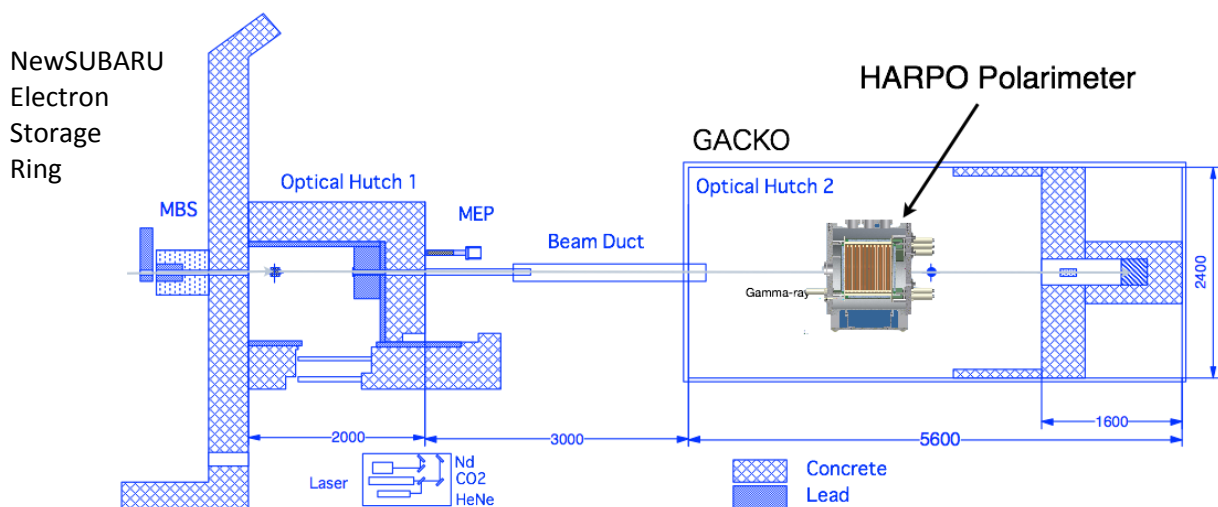
<利用目的>

Test of HARPO, a high angular resolution telescope for gamma-ray polarimetry.
ガンマ線偏光計のための高角度分解望遠鏡HARPOの試験。

<実験方法>

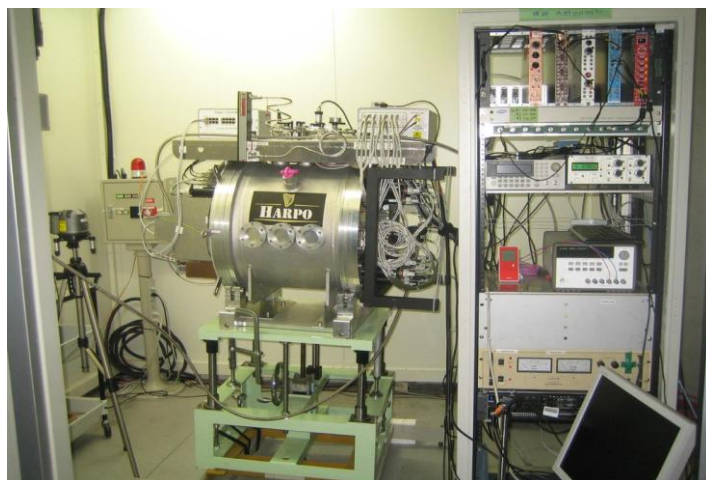
Data were taken at photon energies from 1.7 MeV to 74 MeV, and with different polarisation configurations.

The experimental setup of the TPC and the photon beam are described below.
光子エネルギー1.7MeVから74MeVで異なる偏光条件で、データの取得を行った。
ガンマ線ビームとTPCの実験配置は下図の通り。



文部科学省 [先端研究基盤共用・プラットフォーム形成事業 成果報告]

兵庫県立大学 高度産業科学技術研究所 ニュースバル放射光施設



<実験結果>

The first results from the beam campaign are shown in attached papers.
実験の最初の解析結果の論文を添付する。

<今後の見通し>

This results will use development of HARPO for cosmic gamma-ray polarimeter.
本実験の結果は、宇宙ガンマ線偏光計HARPOの今後の評価・開発のために使われる。

問い合わせ先

兵庫県立大学 高度産業科学技術研究所
ニュースバル放射光施設 共用促進室

〒678-1205 兵庫県赤穂郡上郡町光都1-1-2
TEL : 0791-58-2543 FAX : 0791-58-2504
E-mail : kyoyo@lasti.u-hyogo.ac.jp

the 7th Symposium on Large TPCs for Low-Energy Rare Event Detection,
Paris, 15-17 December (2014).

HARPO: beam characterization of a TPC for gamma-ray polarimetry and high angular-resolution astronomy in the MeV-GeV range

Shaobo Wang

LLR, Ecole Polytechnique, CNRS/IN2P3, France

E-mail: wang@llr.in2p3.fr

**Denis Bernard, Philippe Bruel, Mickael Frotin, Yannick Geerebaert,
Berrie Giebels, Philippe Gros, Deirdre Horan, Marc Louzir,
Patrick Poilleux, Igor Semeniouk**

LLR, Ecole Polytechnique, CNRS/IN2P3, France

David Attié, Denis Calvet, Paul Colas, Alain Delbart, Patrick Sizun

Irfu, CEA-Saclay, France

Diego Götz

AIM, CEA/DSM-CNRS-Université Paris Diderot, France

Irfu/Service d'Astrophysique, CEA-Saclay, France

**Sho Amano, Takuya Kotaka, Satoshi Hashimoto,
Yasuhito Minamiyama, Akinori Takemoto, Masashi Yamaguchi,
Shuji Miyamoto**

LASTI, University of Hyôgo, Japan

Schin Daté, Haruo Ohkuma

JASRI/SPring8, Japan

Abstract. A time projection chamber (TPC) can be used to measure the polarization of gamma rays with excellent angular precision and sensitivity in the MeV-GeV energy range through the conversion of photons to e^+e^- pairs.

The Hermetic ARGON Polarimeter (HARPO) prototype was built to demonstrate this concept. It was recently tested in the polarized photon beam at the NewSUBARU facility in Japan. We present this data-taking run, which demonstrated the excellent performance of the HARPO TPC.

1. Introduction

Gamma-ray astronomy is the primary means by which we can study the non-thermal processes occurring in cosmic sources such as active galactic nuclei (AGN), pulsars and gamma-ray bursts (GRBs) [1]. The ability to measure the linear polarization in this energy range would provide a powerful diagnostic for the understanding of the physical processes at work in these sources [2]. A telescope with the ability to perform polarimetry above 1 MeV has never been flown in space [3]. Gamma-ray telescopes have improved in sensitivity and resolution from COS-B [4] to the Fermi-LAT [5], but the performance of these pair-creation telescopes decreases at low energy where the background is problematic and the angular resolution is limited by multiple scattering.

The performance and polarimetry potential of a TPC have been studied in detail in Ref. [6] and [7]. Several effects contribute to the angular resolution, which is shown as a function of photon energy in Fig. 1 for an argon gas TPC. The angular resolution for pair production is limited by multiple scattering of the electrons in the gas. Also, most conversions take place in the field of a nucleus whose recoil momentum is impossible to measure because of the very short recoil path length. This puts a limit on the resolution at energies < 100 MeV. Even with these limitations however, an improvement in angular momentum of up to an order of magnitude with respect to that of the Fermi-LAT is achievable with a TPC.

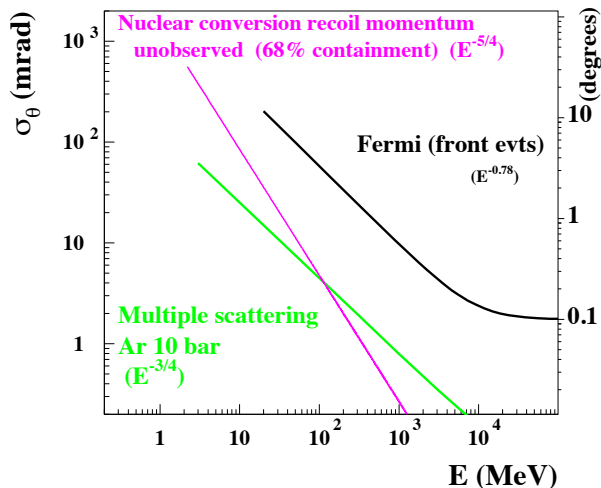


Figure 1. Various contributions to the angular resolution of a TPC gamma telescope as a function of the photon energy [6], compared to that of the Fermi-LAT [5]. The multiple scattering contribution (green) is given for a 10 bar argon TPC, using an optimal tracking such as that implemented in a Kalman filter, and with a track sampling of 1 mm and a spatial resolution of 0.1 mm. At high energies (> 100 MeV), it is limited by the multiple scattering of the electrons in the gas. At lower energies, it is constrained by the unknown recoil momentum of the nucleus. This limit can be overcome by looking at triplet conversion, but they are rarer and more difficult to reconstruct.

The polarimetry of cosmic sources with a pair-creation telescope has long been considered to be difficult or even impossible, as thick, high- Z detector elements are needed to convert the incoming photon, and the conversion electrons then undergo multiple scattering in the converter, after which the information about the azimuthal angle of the conversion plane is blurred [8]. We have built and validated an event generator [7] which is full (5D, either nuclear or triplet conversion) exact down to threshold and polarized. We have characterized the properties of a telescope based on a thin homogeneous detector with optimal tracking and have established

the power laws that describe the dominating contributions to the angular resolution [6]. For such a detector, even when the dilution of the effective polarization asymmetry due to multiple scattering is taken into account, polarimetry can still be performed with high precision (still under the assumption of optimal tracking) [7].

The HARPO project aims to characterize the TPC technology as a high angular resolution polarimeter and telescope in the MeV-GeV range, enabling us to obtain unprecedented sensitivity for the detection of low-energy gamma rays. A TPC is a detector in which traversing charged particles ionize the detector material. The electrons produced drift along an electric field, E , and are then amplified and measured on the x - y readout plane. The drift time gives a measure of the z coordinate. HARPO would be the first space polarimeter above 1 MeV.

In this paper we first describe the demonstrator that we have built to validate the performance of the TPC technology, in particular the characterization of the GEM and micromegas combinations used for gas amplification ¹. Then we present the recent experimental campaign, in which the detector was exposed to the quasi-monochromatic and almost fully polarized beam provided by the BL01 line of the NewSUBARU facility, operated by the LASTI in University of Hyôgo in Japan.

2. The HARPO TPC demonstrator

The HARPO demonstrator [9] (Fig. 2) is a 30 cm cubic TPC which can be operated from low pressure up to 5 bar. It is surrounded by 6 scintillator plates that provide an external trigger. Amplification is performed with the combination of two GEMs [10] and one micromegas [11].

The readout comprises two series (x , y , perpendicular to each other) of 288 copper strips with 1 mm pitch. Signals are acquired with AFTER chips [12] using the Feminos system [13].

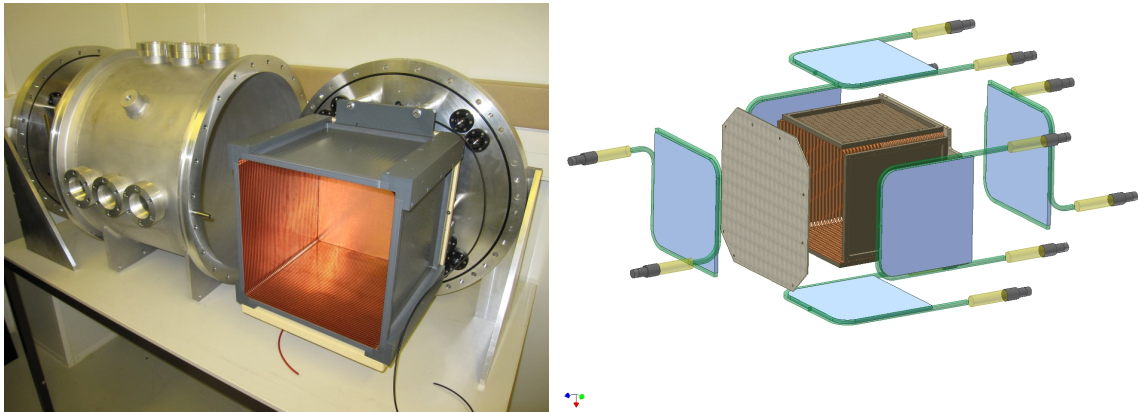


Figure 2. Left: the HARPO TPC demonstrator. Right: sketch of HARPO. A cubic TPC in the center, with a readout plane of micromegas and GEM on the left. Six scintillator plates, each equipped with a wavelength shifter and two photo-multipliers, are used for trigger. The system fits in an aluminum cylinder which can operate up to 5 bar pressure.

¹ The 2012 tests showed that with the 0.4 mm narrow collecting strips that we are using, the micromegas alone does not provide sufficient amplification at 4 bar for routine operation in a safe configuration [9]. We have therefore complemented the micromegas with two layers of Gas Electron Multiplier (GEM).

3. The HARPO amplification system

We first characterized the performance of the GEM+micromegas amplification system using a radioactive source. The amplification system was subsequently integrated into the TPC detector, where it was characterized using cosmic rays.

3.1. Characterization of micromegas and GEM(s) combinations with a radioactive source

We characterized the combination of a micromegas and either one or two GEM in a gas mixture (Ar:95 %Isobutane:5 %) at atmospheric pressure. This was done in a dedicated test setup using a ^{55}Fe source[16]. The successive amplification steps were kept at a distance of 2 mm from each other by spacers (Fig. 3 left).

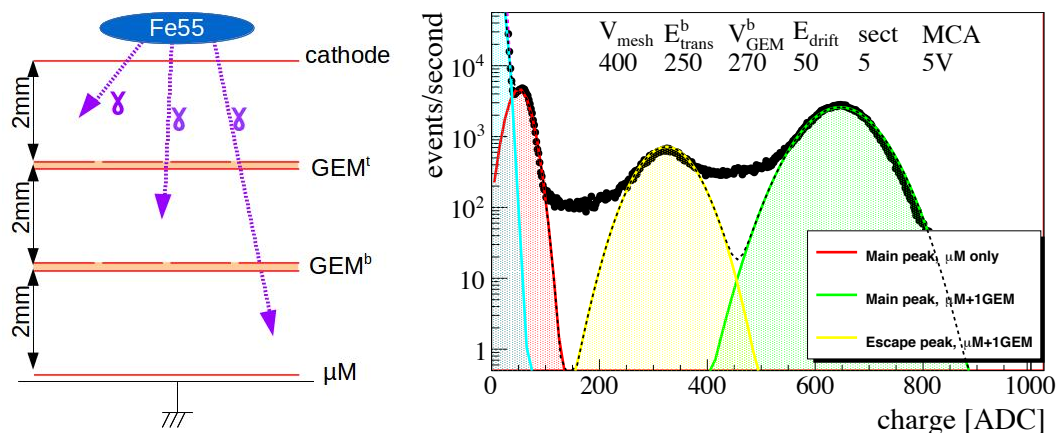


Figure 3. Left: the layout of the test setup, with one micromegas and two GEMs. (By applying a null or inverted voltage to the top GEM, we only observe conversion in the two lower regions). Right: an example of a measured ^{55}Fe spectrum from amplification with one micromegas and one GEM. The main peak (5.9 keV) is plotted after amplification with only the micromegas (red) or with both micromegas and GEM (green). The escape peak is only visible with full amplification (yellow).

In argon, the X-rays from a ^{55}Fe source deposit either 5.9 keV (main peak) or 2.7 keV (escape peak) upon ionization. This conversion can take place either above or below a given GEM sheet. The ionization electrons are therefore either amplified by that GEM or not. A typical spectrum is shown in Fig. 3 (right). The main and the escape peaks are seen with amplification from the micromegas and one GEM, and the main peak with micromegas amplification only. The ratio of the position of the two main peaks provides a precise measurement of the absolute GEM amplification gain. Further details on these measurements, including foil transparency and extraction efficiency, can be found in Ref. [16].

3.2. Characterization with cosmic rays

The system of micromegas and 2 GEMs was commissioned in the detector. It was tested with cosmic rays, using the same gas mixture at several pressures. Most cosmic muons are relativistic and therefore deposit the same average energy per unit length. The TPC was set "vertical", so that most cosmic rays entered it through the amplification system. We selected events with a cosmic ray that crossed the full z of 30 cm by triggering on the coincidence of the up and down scintillator signals.

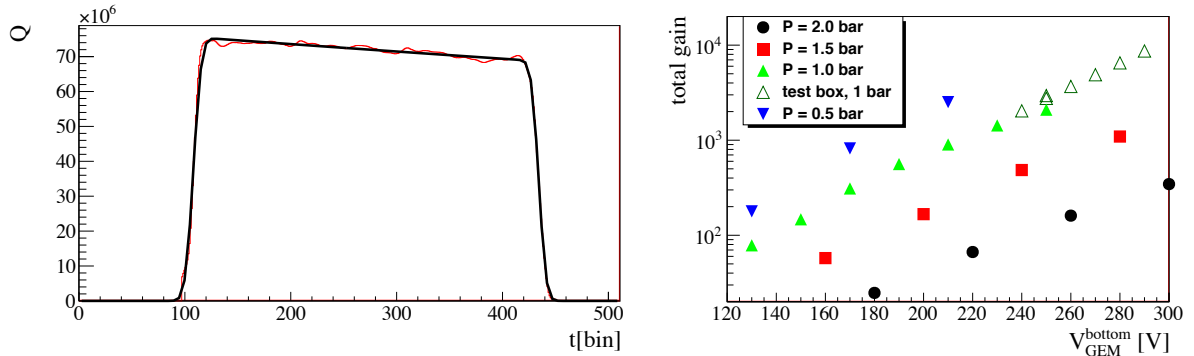


Figure 4. Left: average total charge per track as a function of time, for a run of cosmic rays that traversed the full TPC length, entering through the anode and exiting through the anode. We extract the drift velocity, the electron absorption per unit length and the amplification gain from such spectra. Right: the effective gain measured from cosmic rays in the TPC for several gas pressures. The results at 1 bar are consistent with those obtained with the radioactive source.

Table 1. Electron beam energy, laser wavelength, and γ -ray energy at the Compton edge obtained from these.

E_e^- [GeV]		0.618	0.982	1.233	1.480	Pulsing rate [kHz]	Polarization
Laser	λ [μm]	E_γ [MeV]					
Nd:YVO ₄ (2ω)	0.532	13.4	33.3	52.1	74.3	20	$P \approx 1$
Nd:YVO ₄ (1ω)	1.064	6.76	16.9	26.6	38.1	20	$P \approx 1$
Er(fiber)	1.540	4.68	11.8	18.5	26.5	200	$P = 0$
CO ₂	10.55		1.74	2.73	3.93	CW	$P = 0$

The charge distribution over drift time is shown in Fig. 4 (left). The value of the drift velocity, v_{drift} , was easily obtained using the basic relation of the TPC mechanism, $z = v_{\text{drift}} \times t_{\text{drift}}$, since the cosmic rays traverse the full z thickness of $L_{\text{TPC}} = 30$ cm. The slope of the plateau corresponds to electron absorption in the gas. The average charge per track for each run is used to estimate the amplification gain. From this spectrum, the drift velocity, the attenuation length and the total amplification gain were extracted. Fig. 4 (right) shows the amplification gain for several TPC gas pressures as a function of the voltage on one of the GEMs. The measurements are consistent with those obtained using the ^{55}Fe source.

4. Data-taking at NewSUBARU

In Nov. 2014 the detector was exposed to a beam of pseudo-monochromatic gamma-ray photons delivered by the BL01 beam line at NewSUBARU [15].

4.1. Laser-Compton Source (LCS)

The gamma-ray beam is produced by the inverse Compton scattering of laser photons by relativistic electrons. The electron beam energy can be varied in the range $0.6 \sim 1.5$ GeV. The laser beams available are: Nd:YVO₄ (2ω) with wavelength $\lambda = 0.532 \mu\text{m}$, Nd:YVO₄ (1ω) $\lambda = 1.064 \mu\text{m}$, Er (fiber) $\lambda = 1.540 \mu\text{m}$ and CO₂ $\lambda = 10.55 \mu\text{m}$. This results in a gamma energy range at the Compton edge between 1.7 MeV and 74 MeV as shown in Table 1. As the gamma

has a maximum energy for forward Compton scattering, energy selection was performed by using a collimator on axis. When collimation is applied, the polarisation of the laser beam is almost entirely transferred to the gamma beam: in that way, an almost fully polarized gamma beam ($P \approx 1$) is obtained. A general issue in polarization studies is the control of a possible systematic bias induced by the non-cylindrical-symmetric structure of the detector [17]. Therefore in addition to the fully polarized data, some data with a non polarized beam were taken. To produce such a beam, a $\lambda/4$ plate is used. This changes the linear polarization to circular polarization, which, as far as pair conversion is concerned, is equivalent to random polarization ($P = 0$). Or vice versa.

4.2. The HARPO Trigger system

For the previous characterizations using cosmic rays, the TPC was triggered on a simple coincidence of scintillator signals [9, 14]. In contrast, for data taking in beam, we wished to maximize the fraction of selected gammas that converted in the gas. Therefore a dedicated, more sophisticated trigger was designed. In addition it provides separately the control of the efficiency of each of its components.

4.2.1. Description of signals The HARPO trigger system is based on a PARISROC2 [19] chip mounted on a PMM2 [18] board. This trigger is built from the discriminated signals of the scintillators, laser and micromegas mesh as shown in Fig. 6. The available signals are:

- Laser: when a pulsed laser is used, the laser's trigger signal L (Fig. 5) is used. It also determines the time at which the event takes place, t_0 , with a precision of a few 10 ns.

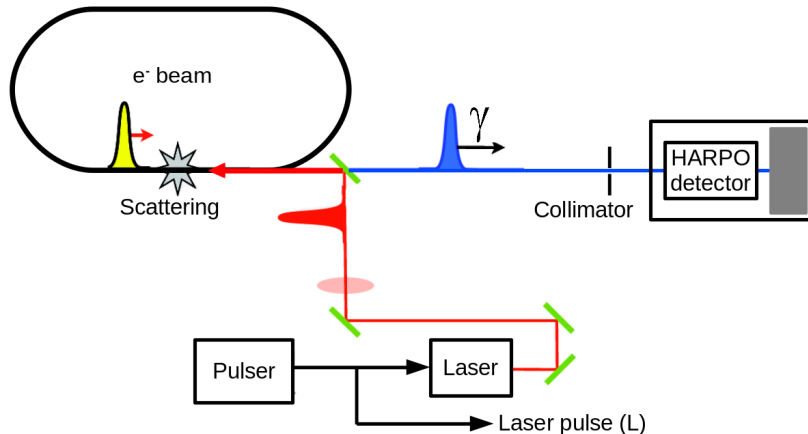


Figure 5. Schema of the Laser trigger used at NewSUBARU.

- Scintillator: the signal comes from 12 PMTs on 6 scintillators. The signal is recorded, whether there is a trigger or not. It gives t_0 with a hundred nanosecond precision. This signal determines t_0 when the laser signal is not available (CO_2).
- Micromegas mesh: the signal induced on the mesh is long and has an unpredictable shape: it corresponds to the time distribution of the charge deposited by the event in the TPC gas as it drifts towards the anode. The signal is amplified and derived through a 5 nF capacitor. It is then discriminated with a constant-fraction discriminator (CFD), so as to determine the rising edge t_{start} of the signal. The RC constant of the readout electronics of the mesh

signal is $\approx 1\mu\text{s}$. It has been fixed as a compromise between the amount of electronic noise given the large capacitance of the full mesh, of 8 nF , and the need of a precise determination of the rising edge of the signal t_{start} .

Events that have a too small of a delay between the time of the event, t_0 , and the discriminated mesh signal rising edge, t_{start} , are rejected. This provides a veto on background tracks created in the beam line upstream of the TPC and on gamma rays which converted in the material between the up scintillator and the active TPC gas (example: in the PCB supporting the amplification system).

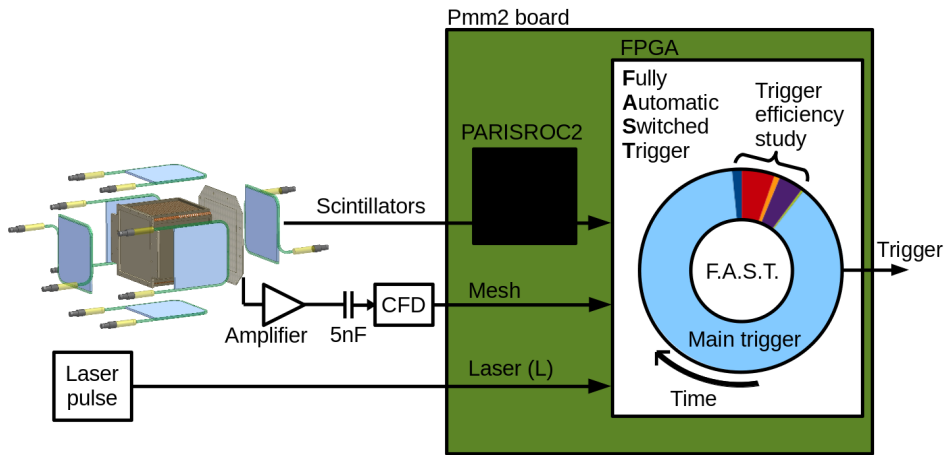


Figure 6. Global view of HARPO trigger system.

4.2.2. Gamma trigger line. The gamma trigger, T_γ , is designed so as to select gamma rays produced by LCS and that converted inside the TPC gas. The conditions are listed below:

- the upstream scintillator signal (S_{up}) is used as a veto,
- at least one downstream scintillator signal (O , other than “up”) is required,
- the laser trigger signal (L), when present, is used,
- the events with a signal present in the mesh are selected, vetoing the prompt part as already explained, we require $t_{\text{start}} - t_0 > 1\mu\text{s}$. This “slow” selection of a mesh signal is denoted M_{slow} .

The main γ trigger line is therefore defined as the combination of the four following components:

$$T_\gamma \equiv \bar{S}_{up} \cap O \cap M_{\text{slow}} \cap L \quad (1)$$

The distribution of t_{start} is shown in Fig. 8. Gamma conversions inside the TPC gas (blue) are the signal events. The flatness of that part of the spectrum is due to the fact that the probability of conversion per unit path length is constant for a thin detector. Tracks entering the detector from upstream and gamma conversions in the detector material upstream of the TPC gas, which escaped the vetos, form the (green) peak. If we had used a trigger without any veto, the height of this peak would have been larger by several orders of magnitude, precluding an efficient data taking. Events (red) which lie outside the normal time range (i.e., $t_{\text{start}} < 100$ or $t_{\text{start}} > 400$) are due to energy deposition inside the gas by events that are not related to the trigger (pile-up).

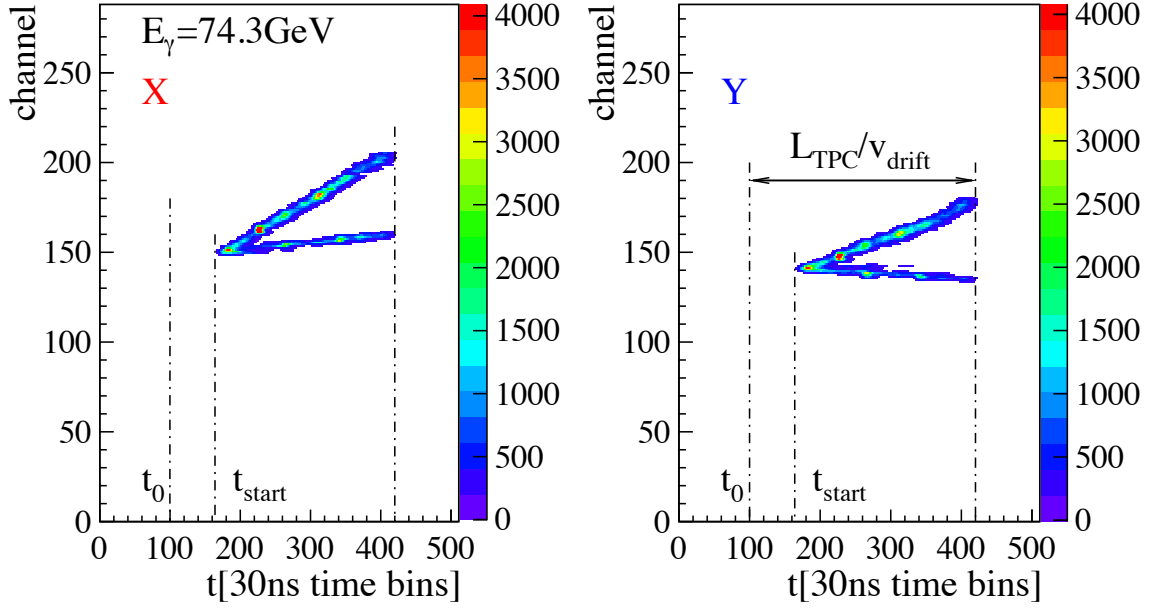


Figure 7. A gamma event that was selected by the gamma trigger, with definitions of timing information.

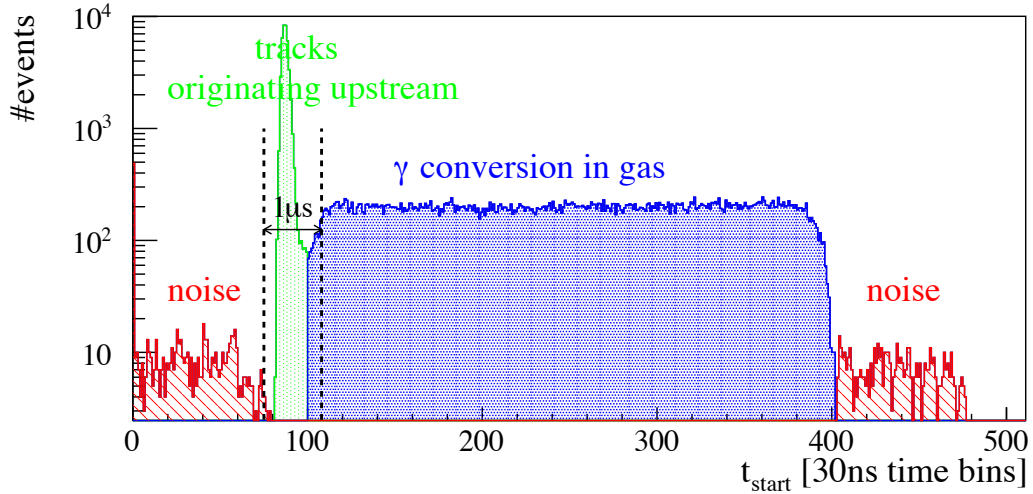


Figure 8. Distribution of event rising edge t_{start} for one run (all trigger lines): tracks originating upstream (green), gamma conversion inside the TPC gas (blue), charge deposition inside the gas by events not related to the trigger (red).

4.2.3. Other Trigger Lines. In addition to the main gamma trigger line, separate trigger lines have been formed with one of the trigger components omitted (such as $O \cap M_{\text{slow}} \cap L$, $\bar{S}_{\text{up}} \cap M_{\text{slow}} \cap L$, $\bar{S}_{\text{up}} \cap O \cap L$, $\bar{S}_{\text{up}} \cap O \cap M_{\text{slow}}$, in the case of a pulsed laser). Analysis of these specific data will enable us to control separately the signal efficiency and the background rejection factor for each component of the main trigger line. Other dedicated lines were used,

such as the “traversing z track” line for calibration purposes. Most of these additional lines were down-scaled so as to not saturate the bandwidth of the digitizing electronics, and were active only for a fraction of the time, as denoted by the rainbow part of Fig. 6. Approximately 90% of the time was devoted to the main trigger line.

4.3. Gas

The pressure vessel was evacuated down to $\sim 2 \times 10^{-6}$ bar, rinsed with ~ 0.1 bar gas, evacuated again, and then filled with 2.1 bar of the gas mixture (Ar:95 % Isobutane:5 %). This same gas was used in a sealed mode for 23 days.

At the end of the data taking, a pressure scan from 1 to 4 bar was performed, with the gas amplification tuned so that the signal amplitude was kept constant ($E_e = 1.5$ GeV, Nd 1ω , $P = 1$).

4.4. Monitoring

During data taking in the beam, some basic parameters were monitored, such as alignment, amplification gain, trigger performance and event quality after some very basic tracking.

4.4.1. Alignment. The alignment of the HARPO detector in the collimated gamma beam was monitored by plotting the transverse (x or y) position of the gamma conversion candidate vertex as a function of its longitudinal position z (Fig. 9). The vertex is defined here from the charge-weighted barycenter of the three first clusters of a selected gamma-conversion event (triggered by the gamma trigger).

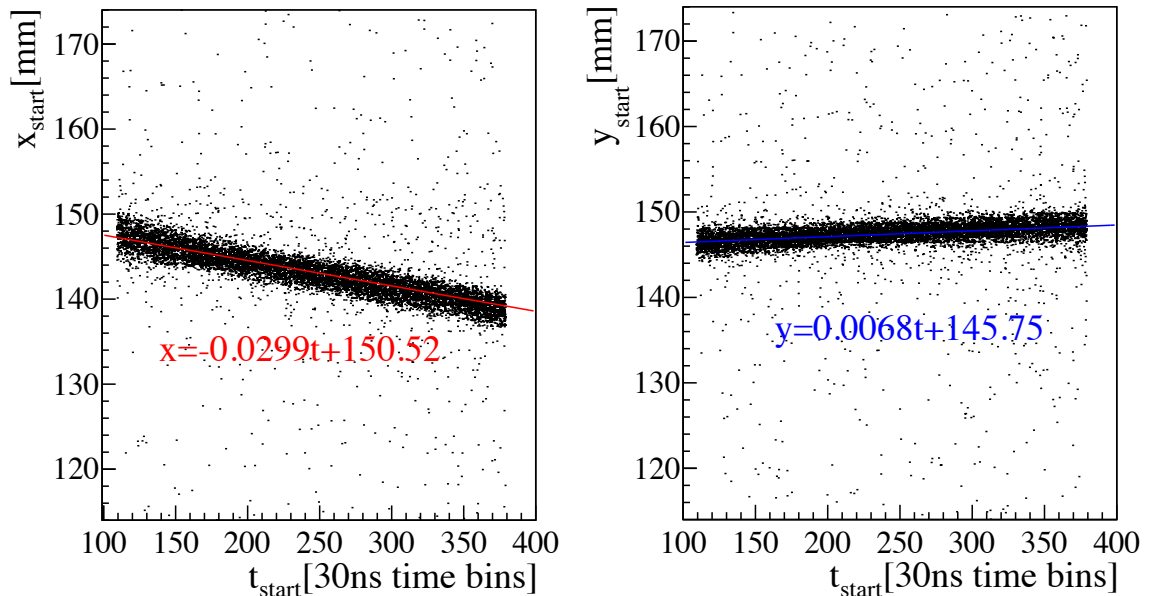


Figure 9. Alignment plot for run 1277 (1 mm diameter collimator), with linear fit (gamma trigger line).

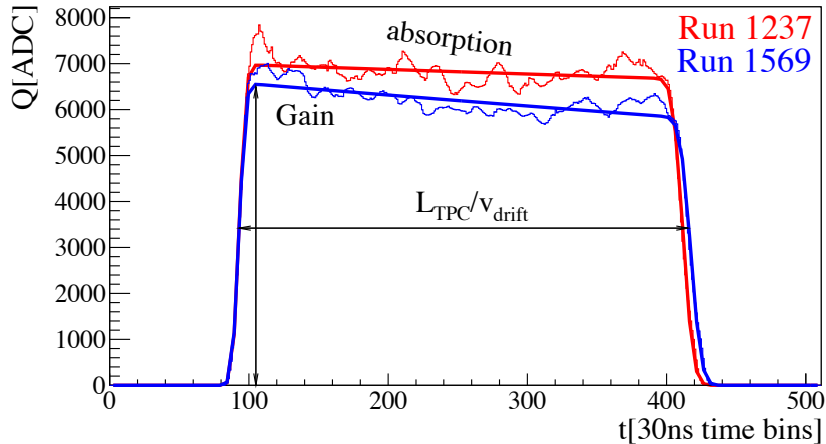


Figure 10. The average energy deposited at each time bin per traversing track along the z -axis for two runs separated by a full week of high flux running.

4.4.2. Calibration. The calibration of the TPC, i.e., the determination of the drift velocity, of the amplification gain and of the electron absorption, is performed by the analysis of the time distribution of the average charge per track as was described in section 3.2. A special trigger line ($\sim 2\%$ of the events) was used to select the tracks traversing in the z direction (i.e., along the drift time) without biasing the time distribution.

Fig. 10 and Fig. 11 show that there was no significant gas deterioration over the two weeks in the beam. The small features that can be seen in the time charts (Fig. 11) are associated with changes in the gamma-beam energy and/or of the laser pulsing rate, meaning that these small biases are related to the measurement, not to the quantity measured. The gas gain and the drift velocity were found to be sufficiently stable and the electron absorption due to either leaks or outgassing was found to be sufficiently small that we didn't have to renew the gas.

5. Conclusions and perspectives

A gas TPC is the instrument suited to covering the performance gap in cosmic gamma-ray detection in the MeV-GeV range. We have built a demonstrator that includes a micromegas+GEM amplification system. We have performed an experimental campaign with this demonstrator using the high-flux, quasi-monochromatic, polarised photon beam at NewSUBARU. Tests that were performed during data taking indicate an excellent detector performance.

We have more than 1 TB of data ($> 6 \times 10^7$ events, a large fraction of which is estimated to be gamma conversions in the gas) to analyze so that we can study the gamma conversion to e^+e^- pairs and, in particular, measure the low energy polarization asymmetry, and characterize the performance of the demonstrator both as a gamma telescope and as a gamma polarimeter. Further development is ongoing to meet the constraints of a space environment [14], in particular, tests on the behaviour of the detector in space with a dedicated trigger. The next step will then be to verify its operation with a balloon flight.

6. Acknowledgments

This work is funded by the P2IO LabEx (ANR-10-LABX-0038) in the framework “Investissements d’Avenir” (ANR-11-IDEX-0003-01) managed by the French National Research Agency (ANR), and directly by the ANR (ANR-13-BS05-0002).

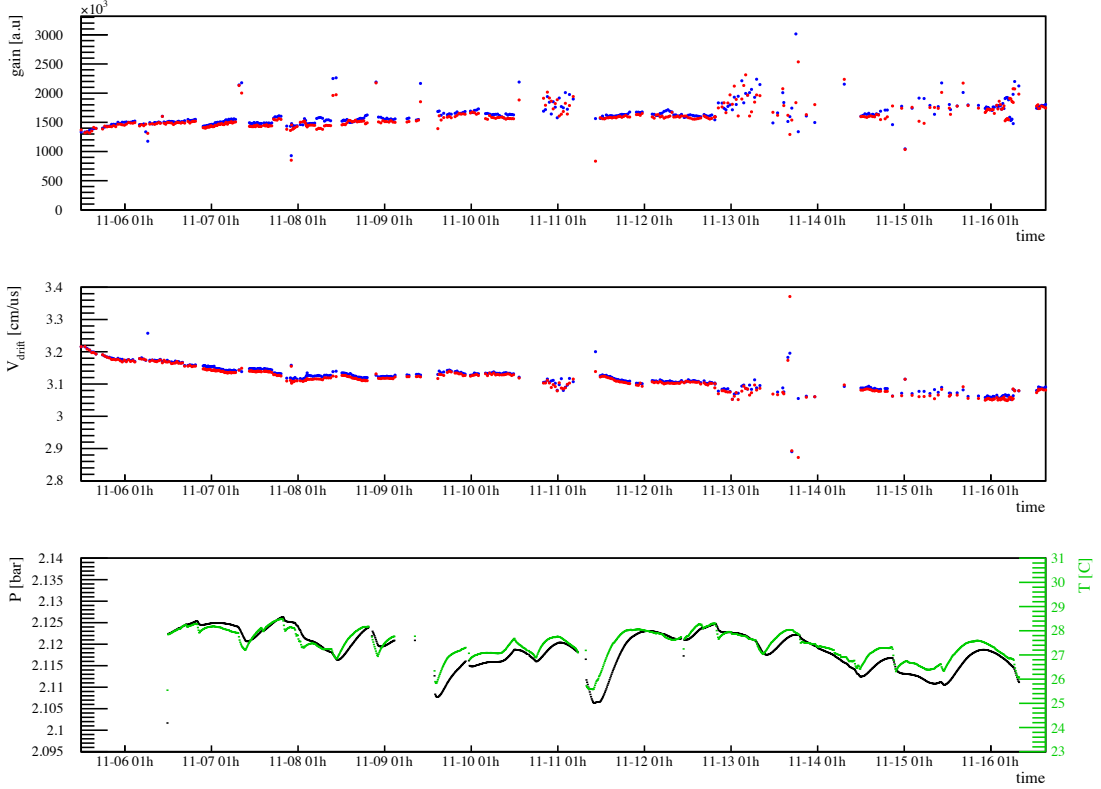


Figure 11. Time variation of the gain, estimated by the average charge per track, corrected for the track angle that is normalized to 30 cm track length, the drift velocity (x in red, y in blue) and the pressure (black) and temperature (green) of the gas.

This work was performed by using NewSUBARU-GACKO (Gamma Collaboration Hutch of Konan University).

References

- [1] D. Eichler, A. Levinson, *Polarization of GRB via scattering off a relativistic sheath*, *Astrophys. J.* **596**, L147 (2003). [astro-ph/0306360].
- [2] H. Zhang and M. Böttcher, *X-Ray and Gamma-Ray Polarization in Leptonic and Hadronic Jet Models of Blazars*, *Astrophys. J.* **774**, 18 (2013) [arXiv:1307.4187 [astro-ph.HE]].
- [3] M. Forot, P. Laurent, I. A. Grenier, C. Gouiffes and F. Lebrun, “Polarization of the Crab pulsar and nebula as observed by the Integral/IBIS telescope,” *Astrophys. J.* **688**, L29 (2008) [arXiv:0809.1292 [astro-ph]].
- [4] H. Bloemen, “Diffuse galactic gamma-ray emission,” *Ann. Rev. Astron. Astrophys.* **27** (1989) 469.
- [5] M. Ackermann *et al.* [Fermi-LAT Collaboration], *The Fermi Large Area Telescope On Orbit: Event Classification, Instrument Response Functions, and Calibration*, *Astrophys. J. Suppl.* **203**, 4 (2012) [arXiv:1206.1896 [astro-ph.IM]].
- [6] D. Bernard, *TPC in gamma-ray astronomy above pair-creation threshold*, *Nucl. Instrum. Meth. A* **701**, 225 (2013) [Erratum-ibid. *A* **713**, 76 (2013)] [arXiv:1211.1534 [astro-ph.IM]].
- [7] D. Bernard, *Polarimetry of cosmic gamma-ray sources above e^+e^- pair creation threshold*, *Nucl. Instrum. Meth. A* **729**, 765 (2013) [arXiv:1307.3892 [astro-ph.IM]].
- [8] Mattox, J. R., Mayer-Hasselwander, H. A., Strong, A. W., *Analysis of the COS B data for evidence of linear polarization of VELA pulsar gamma rays*, *Astrophys. J.* 363 (1990) 270.
- [9] D. Bernard, *HARPO - A Gaseous TPC for High Angular Resolution Gamma-Ray Astronomy and Polarimetry from the MeV to the TeV*, *Nucl. Instrum. Meth. A* **718**, 395 (2013). [arXiv:1210.4399 [astro-ph.IM]].

- [10] F. Sauli, *GEM: A new concept for electron amplification in gas detectors*, Nucl. Instrum. Meth. A **386**, 531 (1997).
- [11] Y. Giomataris, P. Rebourgeard, J. P. Robert and G. Charpak, *MICROMEGAS: A high-granularity position-sensitive gaseous detector for high particle-flux environments*, Nucl. Instrum. Meth. A **376**, 29 (1996).
- [12] P. Baron, D. Calvet, E. Delagnes *et al.*, *AFTER, an ASIC for the readout of the large T2K time projection chambers*, IEEE Trans. Nucl. Sci. **55**, 1744 (2008).
- [13] D. Calvet, “A Versatile Readout System for Small to Medium Scale Gaseous and Silicon Detectors”, IEEE Transactions on Nuclear Science 61 (2014) 675.
- [14] D. Bernard *et al.*, Presented at SPIE2014. Proc SPIE 9144 M. [arXiv:1406.4830 [astro-ph.IM]].
- [15] S. Amano *et al.*, *Several-MeV γ -ray generation at NewSUBARU by laser Compton backscattering*, Nucl. Instrum. Meth. A **602** 2009 337.
- [16] Ph. Gros, *HARPO - TPC for High Energy Astrophysics and Polarimetry from the MeV to the TeV*, TIPP 14 3rd Technology and Instrumentation in Particle Physics conference, 2-6 June 2014 Amsterdam, Proceedings PoS(TIPP2014)133.
- [17] M. Weisskopf, *X-ray Polarimetry: from the early days to an outlook for the future*, X-ray polarisation in astrophysics, August 25-28, Stockholm, Sweden.
- [18] B. Genolini *et al.*, *PMm2: Large photomultipliers and innovative electronics for the next-generation neutrino experiments*, Nucl. Instrum. Meth. A **610** (2009) 249 [arXiv:0811.2681 [physics.ins-det]].
- [19] S. Conforti Di Lorenzo *et al.*, *PARISROC, an autonomous front-end ASIC for triggerless acquisition in next generation neutrino experiments*, Nucl. Instrum. Meth. A **695** (2012) 373.

HARPO, a gaseous TPC as a gamma telescope and polarimeter: first measurement in a polarised photon beam between 1.7 and 74 MeV

A. Delbart*

Irfu, CEA-Saclay, Gif-sur-Yvette, France

E-mail: alain.delbart@cea.fr

**S. Amano^b, D. Attié^a, D. Bernard^c, P. Bruel^c, D. Calvet^a, P. Colas^a, S. Daté^d,
M. Frotin^c, Y. Geerebaert^c, B. Giebels^c, D. Götz^{ae}, P. Gros^c, S. Hashimoto^b,
D. Horan^c, T. Kotaka^b, M. Louzir^c, Y. Minamiyama^b, S. Miyamoto^b, H. Ohkuma^d,
P. Poilleux^c, I. Semeniouk^c, P. Sizun^a, A. Takemoto^b, S. Wang^c, M. Yamaguchi^b,**

^a *Irfu, CEA-Saclay, Gif-sur-Yvette, France*

^b *LASTI, University of Hyogo, Japan*

^c *LLR, Ecole Polytechnique, CNRS/IN2P3, Palaiseau, France*

^d *JASRI/SPring8, Japan*

^e *AIM, CEA/DSM-CNRS-Université Paris Diderot, France*

Gamma-ray astronomy enables the exploration of the non-thermal emission and magnetic field configuration of objects such as active galactic nuclei (AGN), gamma ray bursts (GRB) and pulsars. Presently, there is a sensitivity gap between 1 MeV and 100 MeV. Additionally, there is no polarisation measurement above 1 MeV, although such a measurement could shed light on emission processes. A gaseous detector can achieve a much better angular resolution in the MeV-GeV range than the current/past telescopes that use tungsten converters, thanks to the reduced multiple scattering of the electrons and positrons. This translates to a greatly improved point source sensitivity and gives access to the linear polarisation of the photons through the azimuthal angle of the pair.

The HARPO time projection chamber (TPC) is a high angular resolution telescope for gamma-ray polarimetry. It was installed in a polarised gamma-ray beam at NewSUBARU in Japan in 2014. Data were taken at photon energies from 1.7 MeV to 74 MeV, and with different polarisation configurations. The experimental setup of the TPC and the photon beam are described. The first results from the beam campaign are shown.

The 34th International Cosmic Ray Conference,

30 July- 6 August, 2015

The Hague, The Netherlands

*Speaker.

1. Science case

High-energy photons such as γ -rays emitted by cosmic sources are produced by non-thermal phenomena that involve high-energy charged particles. They provide unique information on the processes at work in objects such as active galactic nuclei (AGN), pulsars and gamma-ray bursts (GRB). Presently γ -ray astronomy suffers from a gap in sensitivity between the energy ranges in which Compton telescopes (sub-MeV), and e^+e^- -pair telescopes (above 1 GeV) excel. In principle, pair telescopes could be sensitive down to threshold, but in practice the bad angular resolution at low energy hinders their ability to assign a given photon to a particular source. This situation is detrimental to the understanding of objects that have a multi-peak spectral energy distribution (SED), such as AGN, and to objects whose emission is peaking in the MeV region (the prompt emission of many GRB). A better sensitivity is also needed to track high-energy cosmic-rays from super-nova remnants (SNR) from their hadronic interactions, by the detection of the π^0 bump at ≈ 100 MeV. An improved angular resolution is needed to observe crowded regions of the γ -ray sky, such as in the centre of our galaxy.

At low photon energies, from radio-waves to soft-X-rays, polarimetry provides a powerful insight to phenomena at work inside cosmic sources, in particular it provides a means to measure the magnetic field. Above a couple of MeV, this diagnostic is missing: not only does the Compton cross section decrease at high energy, but its polarisation asymmetry also decreases, like $1/E$ [1]. Polarimetry would allow, for example, to decipher leptonic from hadronic models of blazars [2]. In the case of a γ -ray production by synchrotron emission of high-energy protons, the linear polarisation fraction stays high from X-ray to γ -ray energies. In the case of “leptonic” emission though, X-ray emission is highly polarised, but the γ -ray part of the spectrum is completely washed out by the inverse Compton scattering of thermal photons, and the total emission is unpolarised. Polarimetry is also of interest for searches of Lorentz invariance violation (LIV) using GRB [3]. In the presence of LIV, the induced birefringence of the vacuum would result in an energy-dependent rotation of the polarisation direction of a (supposedly) initially polarised emission, upon propagation. On average this would result to an unpolarised radiation: if a non-zero polarisation of distant GRB is observed, an upper limit on LIV-producing effects by yet-unknown physics beyond the standard model is derived [3]. As the rotation angle is proportional to the squared photon energy, extending polarimetry to the γ -ray energy range would enable a huge gain in sensitivity.

2. Telescope and polarimeter with a thin homogeneous detector and an optimal tracking

Past and presently active pair telescopes use an active target that consists of a “mille-feuille”, a multi-layer set of alternatively high- Z converter slabs and sensor foils. In the case of the Si/W tracker of the Fermi/LAT, the single photon angular resolution is dominated by the multiple scattering of the electrons in the slabs and scales like $E^{-0.78}$ below 10 GeV, and amounts to $\approx 4^\circ$ at 100 MeV [4]. Doing better with this technology would involve thinner and/or lower- Z converters, a severe issue for space missions for which the number of electronic channels is limited. A way out is the use of a low-density (here gas) detector such as a time projection chamber (TPC), a detector widely used in particle physics: a volume of (here homogeneous) material is immersed in a

(here uniform) electric field. Upon occurrence of an “event”, that is of the conversion of a photon to an e^+e^- pair, the two tracks ionise the gas after which the ionisation electrons drift towards an anode where they are amplified, collected and sampled in time. A segmented anode provides a time “map” of the signal over the two directions x and y transverse to the electric field. Time sampling provides a measurement of the drift duration, that is of the drift length z . In total a 3D image of the event is provided at a reasonable cost in terms of number of electronics channels. The single-photon angular resolution includes several contributions:

- **Recoil.** In the case of a “nuclear” conversion, that is a conversion by interaction of the photon with the field of a nucleus of the detector, the energy that is transferred to the nucleus is small and the track length is too short to be reconstructed. The contribution of the recoil momentum to the reconstructed momentum of the photon is therefore missing. Given the high-momentum tail of the recoil momentum distribution (Fig. 3 of [5]), we have estimated the contribution to the angular resolution by the angle that includes 68 % of the events [5] to be $\approx 1.5 \text{ rad}(E/1\text{MeV})^{-5/4}$.

Triplets. In the case of the conversion in the field of an electron of the detector, the track of the recoiling electron can be long enough that it can be reconstructed, in which case its contribution can be taken into account in the reconstruction: the event is then called a “triplet”, as three tracks are visible in the final state. Unfortunately these events are too few to contribute significantly to the differential sensitivity (slide 20 of [6]). As the azimuthal angle of the recoil is correlated with the direction of polarisation of the incident photon, hope has raised to perform polarimetry with triplet ([7] and references therein). Alas, the cross section above a threshold recoil momentum gets low at low photon energy (Fig. 6 of [8]), and in total the potential of triplet for polarimetry is quite limited (section 5.3 of [8]).

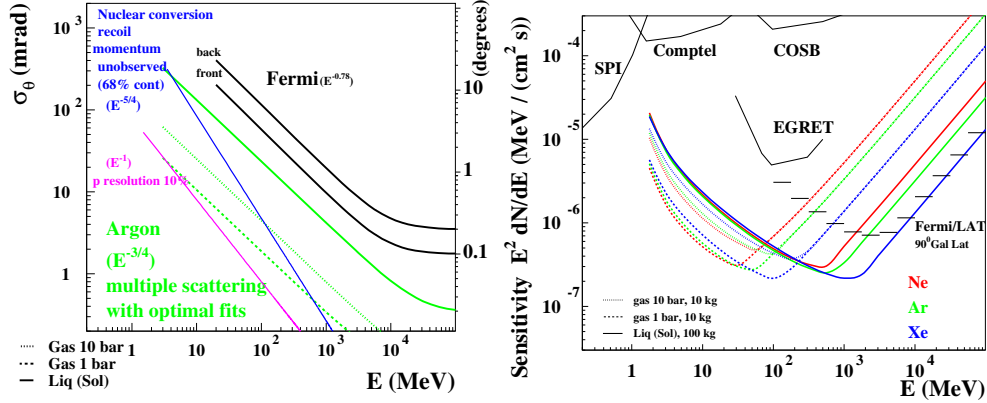


Figure 1: (Colour online). Left: various contributions to the photon angular resolution; Right: point-like source differential sensitivity [5].

- Next comes the multiple scattering of the tracks in the TPC material. These angular deflections induce correlated deviations between successive position measurements of a track, that must be taken into account in the reconstruction. It can be shown that this can be performed in an optimal way by a Kalman-filter-based fitter [9]. In that case, in the continuous detector

limit [10], the expression of the RMS track angular resolution at its starting point is [5, 8] $\sigma_{\theta tL} = (p/p_1)^{-3/4}$, where p is the track momentum, $p_1 \equiv p_0 (4\sigma^2 l/X_0^3)^{1/6}$ is a characteristic momentum that parametrises the performance of the tracking under multiple-scattering of a given detector, and $p_0 = 13.6 \text{ MeV}/c$ is the constant that appears in the expression of multiple scattering (eq. (32.15) of [11]). In the expression for p_1 , σ is the single-point spatial resolution, l is the track longitudinal sampling, and X_0 is the radiation length of the tracker material. The single-track angular resolution is extended easily to the average single-photon angular resolution by multiplication by a factor that is close to unity [5]. The $p^{-3/4}$ variation compares nicely with the experimental value of $E^{-0.78}$ for the Fermi/LAT collaboration [4]. For $l = 1 \text{ mm}$, $\sigma = 0.1 \text{ mm}$ and a 10 bar argon-based gas, $\sigma_{\theta tL} = 0.26^\circ$ at $E = 100 \text{ MeV}$, while the recoil contribution amounts to 0.27° (Fig. 1), The two curves cross close to 100 MeV, and the total angular resolution amounts to 0.4° at 100 MeV, which is an order of magnitude improvement with respect to the Fermi/LAT. The expression for $\sigma_{\theta tL}$ was cross-checked with an actual Kalman-filter (Fig. 18 of [8]).

- **Detector resolution.** At the highest energy, the angular resolution flattens to an asymptote dominated by the detector resolution (Fig. 1 left).
- **Momentum resolution.** Track momentum can be measured either directly in the TPC, if immersed into a magnetic field, or with additional external detectors such as a transition radiation detector (TRD) or a calorimeter. For the lowest energies, the momentum can be estimated by the multiple measurement of multiple scattering in the TPC alone ([5] and references therein). For a 10 % resolution, the contribution to the photon angular resolution is negligible (Fig. 1 left).

The improvement in angular resolution translates to an improvement in point-like source differential sensitivity, as is shown in Fig. 1 right. Indeed, together with the high-performance Compton-telescope projects presently under development, closing the sensitivity gap is within reach.

Polarimetry has long been considered to be out of reach for e^+e^- -pair telescopes as multiple scattering blurs the azimuthal angular information, that between the conversion plane and a direction transverse to the propagation of the photon. Following the approximation of [12], that is an opening angle between the e^+e^- pair equal to its most probable value, the resolution for the azimuthal angle is independent of photon-energy. In a mille-feuille telescope, after a path length of $\approx 10^{-3}X_0$ in the conversion slab, the polarisation asymmetry already undergoes a dilution of the polarisation asymmetry of a factor of two [8]. In a homogeneous detector though, the resolution for the azimuthal angle varies like $E^{1/4}$ (eq. (18) of [8]): there is hope that in the lower part of the energy spectrum of a pair telescope, where most of the statistics lies, the dilution stays high¹. We have written an event generator which samples from the full, 5D, differential cross section, exact down to threshold. It does not rely on any high-energy approximation, and includes polarisation [8]. We have used it to study the performance of an homogeneous tracker with optimal tracking as described above, using the full 5D event probability density function (pdf). We found that for a gas TPC the dilution stays indeed very close to unity over most of the energy spectrum (Fig. 20 of [8]).

¹We are using the high-energy physics definition of the dilution D of the asymmetry \mathcal{A} , that is $D \equiv \mathcal{A}_{\text{eff}}/\mathcal{A}$, that is the higher the value of D , the better.

With a 1 m^3 5 bar argon TPC, one full (exposure fraction of $\eta = 1$) year exposure to a Crab-like source and with experimental cuts applied, a P precision of 1.4% would be reached [8].

3. HARPO: the detector

The HARPO demonstrator is a 30 cm cubic TPC surrounded by 6 scintillator plates equipped with a wavelength shifter and two photomultipliers (PMTs) for trigger and background rejection. The gas container vessel is an aluminum cylinder designed to be operated from few mbar up to 5 bar in sealed mode (Fig. 2). The TPC is filled with a mixture of argon with 5% of $i\text{C}_4\text{H}_{10}$ and operated with a 220 V/cm drift electric field. The TPC end-plate is a "hybrid" MicroPattern Gaseous Detector (MPGD) which is composed of two GEM foils [13] stacked with 2 mm spacing above a $128 \mu\text{m}$ amplification gap bulk-micromegas [14]. The anode collection plane is segmented in 2 times 288 strips in the two orthogonal $x - y$ directions read by an electronic chain composed of two T2K/TPC Front-End cards, two FEMINOS back-end cards and a Trigger Clock Module [15]. An innovative trigger system, called FAST (Fully Automated Switched Trigger), makes use of the FPGA of a modified PMm2 trigger card to sequentially generates up to 16 trigger lines built with combinations of the signals from the 12 PMTs, micromegas mesh signal, and an external laser trigger. This demonstrator was extensively studied in laboratory with a ^{55}Fe 5.9 keV X-ray source and with cosmic rays to measure its performances and determine its operating conditions [16].

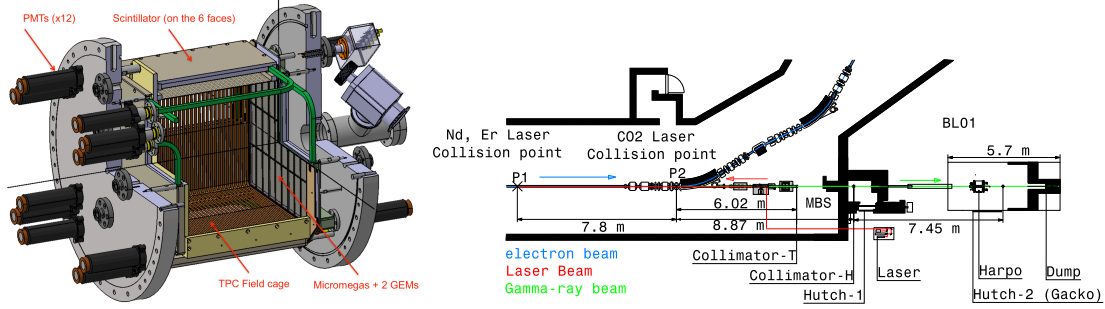


Figure 2: Left: a 3D CAD drawing of the HARPO demonstrator; Right: the gamma beam line and test setup at NewSUBARU.

4. Detector test with a polarised gamma-ray beam

In November 2014, the HARPO demonstrator was exposed to a pseudo-monochromatic and almost fully polarised γ -ray beam delivered by the BL01 beam line of the NewSUBARU storage ring [17] (figure 2) which is operated by the Laboratory of Advanced Science and Technology for Industry (LASTI) of the University of Hyôgo (Japan). The γ -ray beam is produced by the inverse Compton scattering of laser photons on the relativistic electrons stored in NewSUBARU (Laser Compton Source or LCS). We used four electron beam energies: 0.618, 0.982, 1.223 and 1.480 GeV. We could cover the γ -ray energy range from 1.74 MeV up to 74.3 MeV through four available laser photon wavelengths: $\lambda = 0.532 \mu\text{m}$ and $\lambda = 1.064 \mu\text{m}$ with a 20 kHz

pulsed Nd:YVO₄ (2ω and 1ω) laser, $\lambda = 1.540\mu\text{m}$ with a 200kHz pulsed Er (fibre) laser and $\lambda = 10.55\mu\text{m}$ with a CW CO₂ laser (Fig. 5). In order to select the Compton energy edge, we used two 100 mm long collimators made of lead bricks and that we precisely aligned on the beam axis by γ -ray energy measurements with a NaI detector. When collimation is applied, the laser beam linear polarisation (measured to be above 99.9%) is almost fully transferred to the γ -ray beam. For systematic bias studies, the laser beam was also changed to circular polarisation by use of a quarter-wave plate, which, for an experiment that is not sensitive to the polarisation of the leptons, is equivalent to random polarisation ($P = 0$).

The HARPO demonstrator was filled with gas at 2 bar after successive vacuum pumpings and rinsings. The main effects of gas degradation are a modification of the amplification gain and a loss of signal due to capture of electrons along the drift. Figure 3 shows a measure of the relative gain and electron drift velocity over the two weeks of data taking, with a slight variation of gain and drift velocity (around 5%). A monitoring of the temperature and pressure shows that we had a very low leakage rate.

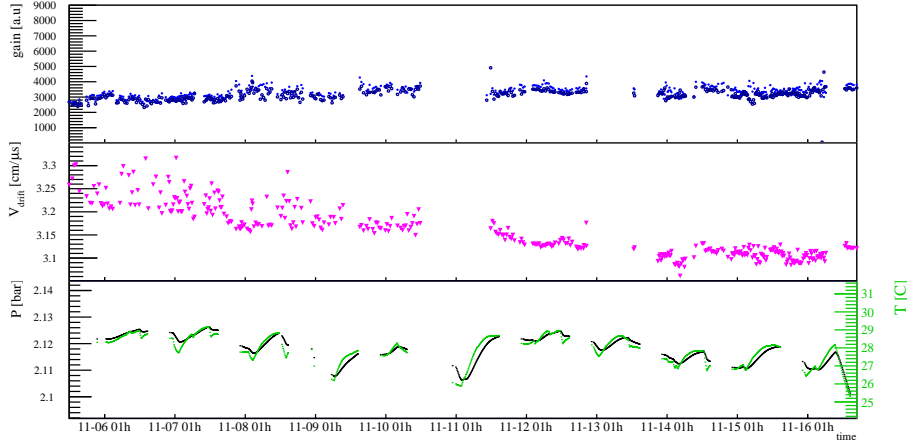


Figure 3: Evolution of the gain, electron drift velocity, temperature and pressure during data taking.

A special trigger line was developed for selecting γ -ray from LCS conversion in the gas. It uses the signal of the 6 scintillators, the start signal from the pulsed laser, and the signal from the micromegas mesh. It was designed to select events with conversion in the TPC gas, while rejecting conversions in the upstream material. This was done by applying a veto on "early" signals in the mesh, which come from electrons with zero or short drift. This trigger system is suitable for a configuration in beam and not for a space telescope. Additional trigger lines were included to check the efficiency of the different trigger elements. Figure 4 shows a selection of conversion events. Our raw output is a pair of 2D maps, representing the $x-z$ and $y-z$ projections, where z is obtained from the arrival time of the electrons. In most cases, we see nuclear conversion, where only the e^+e^- pair is visible. Occasionally, we see triplet conversions, where the recoil electron forms a third track. An estimation of the rate of gamma conversions in the gas comes from looking at the position of the "start" (i.e. z/t minimum, the point closest to the beam side) of an event. This point is an approximation of the vertex position (Fig. 4). If that point is within the transverse geometrical location of the γ -ray beam and longitudinal location of the TPC gas, we estimate that

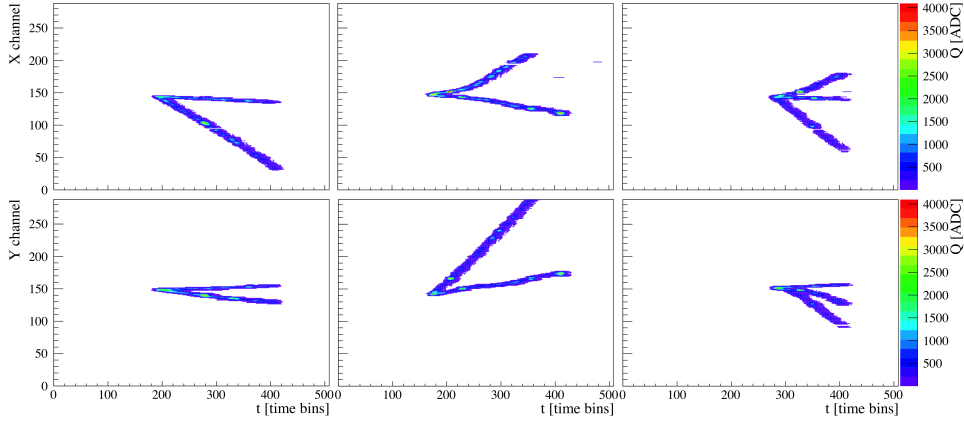


Figure 4: Raw data from 3 pair conversion events. Left : a 74.3 MeV photon; Middle : a 4.68 MeV photon. Right : a 74.3 MeV photon with recoil electron (triplet conversion). The top and bottom represent the $x - z$ and $y - z$ projections. The signal is spread out by diffusion and electronics shaping. This will be taken into account in the reconstruction algorithms.

the event contains an interaction of the beam with the gas. Figure 5 shows how this selection is done, and gives the estimated fraction of recorded events which show interactions of γ -rays in the gas volume. The rate of acquisition of gamma events reached up to 50 Hz for a total of nearly 60 million events, so that at least 30 million events are due to an interaction of the photons with the gas. At the considered energies, most of these events should be pair conversions.

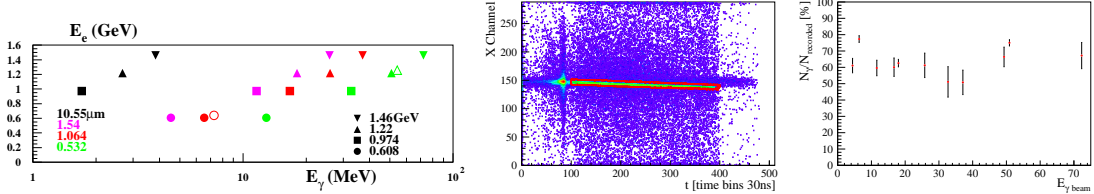


Figure 5: Left: γ energies as a function of electron energies and laser wavelengths; Middle: distribution of the position of the first signal in the TPC for each event in one run. The central region (in red) represents the beam position. Events in that region are considered to contain an interaction of the γ -rays with the gas; Right: resulting fraction of all recorded events which contain γ -rays for most of the photon energies used.

5. Conclusion and Perspectives

The HARPO TPC demonstrator was exposed to polarised gamma photons with energies between 1.74 MeV and 74.3 MeV. The data taking was efficient with more than 50% of high quality events coming from gamma conversion to e^+e^- pairs inside the TPC gas volume. A complete reconstruction and characterisation of these events is on-going to measure the angular resolution of the detector, as well as its sensibility to the photon polarisation. In the perspective of a stratospheric balloon flight test, several R&D programs are on-going on the design of a rad-hard electronics, the

optimization of the MPGD by use of a thin gap micromegas optimised for high pressure, and the development of an advanced trigger and a gas recirculation system.

6. Acknowledgements

This work is funded by the French National Research Agency (ANR-13-BS05-0002) and was performed by using NewSUBARU-GACKO (Gamma Collaboration Hutch of Konan University).

References

- [1] D. Bernard, *Compton polarimetry revisited*, arXiv:1507.02824 [astro-ph.IM].
- [2] H. Zhang and M. Böttcher, *X-Ray and Gamma-Ray Polarization in Leptonic and Hadronic Jet Models of Blazars*, *Astrophys. J.* **774**, 18 (2013) [arXiv:1307.4187 [astro-ph.HE]].
- [3] D. Götz *et al.*, *GRB 140206A: the most distant polarized Gamma-Ray Burst*, *Mon. Not. Roy. Astron. Soc.* **444** (2014) 3, 2776 [arXiv:1408.4121 [astro-ph.HE]].
- [4] M. Ackermann *et al.*, *The Fermi Large Area Telescope On Orbit: Event Classification, Instrument Response Functions, and Calibration*, *ApJS* **203** (2012) 4, [arXiv:1206.1896 [astro-ph.IM]].
- [5] D. Bernard, *TPC in gamma-ray astronomy above pair-creation threshold*, *Nucl. Instrum. Meth. A* **701** (2013) 225 [*Nucl. Instrum. Meth. A* **713** (2013) 76] [arXiv:1211.1534 [astro-ph.IM]].
- [6] D. Bernard, *A thin detector as a high angular resolution gamma ray telescope (and polarimeter) in the MeV-TeV energy range; Towards a post-Fermi mission ?* Gamma2012, 5th International Symposium on High-Energy Gamma-Ray Astronomy, Heidelberg, July 9-13 2012.
- [7] V. F. Boldyshev *et al.*, *Measurement of linear polarization of photons by using the asymmetry of recoil electrons in the photoproduction of triplets*, *Phys. Atom. Nucl.* **58** (1995) 39 [*Yad. Fiz.* **58** (1995) 43].
- [8] D. Bernard, *Polarimetry of cosmic gamma-ray sources above e^+e^- pair creation threshold*, *Nucl. Instrum. Meth. A* **729** (2013) 765 [arXiv:1307.3892 [astro-ph.IM]].
- [9] R. Frühwirth, *Application of Kalman filtering to track and vertex fitting*, *Nucl. Instrum. Meth. A* **262**, 444 (1987).
- [10] W. R. Innes, *Some formulas for estimating tracking errors*, *Nucl. Instrum. Meth. A* **329**, 238 (1993).
- [11] K. A. Olive *et al.* [Particle Data Group Collaboration], *Review of Particle Physics*, *Chin. Phys. C* **38** (2014) 090001.
- [12] Yu. D. Kotov, *Methods of measurement of gamma-ray polarization*, *Space Science Reviews* 49 (1988) 185.
- [13] F. Sauli, *GEM: A new concept for electron amplification in gas detectors*, *Nucl. Instrum. Meth. A* **386**, (1997) 531.
- [14] I. Giomataris *et al.*, *Micromegas in a bulk*, *Nucl. Instrum. Meth. A* **560**, (2006) 405.
- [15] D. Calvet, *A Versatile Readout System for Small to Medium Scale Gaseous and Silicon Detectors*, *IEEE Trans. Nucl. Sci.* **61** (2014) 675.
- [16] S. Wang *et al.*, *HARPO: beam characterization of a TPC for gamma-ray polarimetry and high angular-resolution astronomy in the MeV-GeV range*, [arXiv:1503.03772 [astro-ph.IM]].
- [17] S. Amano *et al.*, *Several MeV γ -ray generation at NewSUBARU by laser Compton backscattering*, *Nucl. Instrum. Meth. A* **602** (2009) 337.

Measurement of 1.7 to 74 MeV polarised γ rays with the HARPO TPC

Y. Geerebaert^{a,*}, Ph. Gros^{a,*}, S. Amano^e, D. Attié^b, D. Bernard^a, P. Bruel^a, D. Calvet^b, P. Colas^b, S. Daté^f, A. Delbart^b, M. Frodin^a,
B. Giebels^a, D. Götz^{c,d}, S. Hashimoto^e, D. Horan^a, T. Kotaka^e, M. Louzir^a, Y. Minamiyama^e, S. Miyamoto^e, H. Ohkuma^f,
P. Poilleux^a, I. Semeniouk^a, P. Sizun^b, A. Takemoto^e, M. Yamaguchi^e, S. Wang^a

^aLLR, École Polytechnique, CNRS/IN2P3, Palaiseau, France

^bCEA, Irfu, CEA-Saclay, France

^cAIM, CEA/DSM-CNRS-Université Paris Diderot, France

^dIRFU/Service d'Astrophysique, CEA-Saclay, France

^eLASTI, University of Hyogo, Japan

^fJASRI/SPring8, Japan

Abstract

Current gamma-ray telescopes based on photon conversion to electron-positron pair, such as Fermi, use tungsten converters. They suffer of limited angular resolution at low energies, and their sensitivity drops below 1 GeV. The low multiple scattering in a gaseous detector gives access to higher angular resolution in the MeV-GeV range, and to the linear polarisation of the photons through the azimuthal angle of the electron-positron pair.

HARPO is an R&D program to characterize the operation of a TPC (Time Projection Chamber) as a high angular-resolution and sensitivity telescope and polarimeter for γ -rays from cosmic sources. It represents a first step towards a future space instrument.

A 30 cm cubic TPC demonstrator was built, and filled with 2 bar argon based gas. It was put in a polarised gamma-ray beam at the NewSUBARU accelerator in Japan in November 2014. Data were taken at different photon energies from 1.7 MeV to 74 MeV, and with different polarisation configurations.

The electronics setup is described, with an emphasis on the trigger system. The event reconstruction algorithm is quickly described, and preliminary measurements of polarisation of 11 MeV-photons are shown.

Key words: TPC, gamma-ray, polarimetry, gaseous detector

1. High angular resolution γ -ray astronomy and polarimetry in the MeV - GeV energy range

γ -ray astronomy provides insight to the understanding of the non-thermal emission of among the most violent objects in the Universe, such as pulsars, active galactic nuclei (AGN) and γ -ray bursts (GRB), and thereby to the understanding of the detailed nature of these objects.

Alas, between the sub-MeV and the above-GeV energy ranges for which Compton telescopes ($\gamma e^- \rightarrow \gamma e^-$) and pair telescopes ($\gamma Z \rightarrow Ze^+e^-$) are, respectively, highly performant, lies the MeV-GeV range over which the sensitivity of past measurements was very limited, in particular as the degradation of the angular resolution of pair telescopes at low energy ruins the detection sensibility. This hinders the observation and the understanding of GRBs, the spectrum of most of which peaks in the MeV region, it biases the description of the Blazar sequence. More generally, it limits the detection of crowded regions of the γ -ray sky such as the galactic plane to its brightest sources : to a large extent, the MeV-GeV sensitivity gap [1] is an angular resolution issue.

The angular resolution of pair telescopes can be improved, from the Fermi/LAT's $\approx 5^\circ$ at 100 MeV [2] to $1 - 2^\circ$, by the use of pure silicon trackers, i.e. without any tungsten converter plates [3, 4, 5]. An even better resolution of $\approx 0.4^\circ$ can be obtained with a gas detector such as a time-projection chamber (TPC), such that together with the development of high-performance Compton telescope, filling the sensitivity gap for point-like sources at a level of $\approx 10^{-6}$ MeV/(cm²s) is within reach [6] and Fig. 1.

Furthermore the measurement of the linear polarization of the emission, which is a powerful tool to understand characteristics of cosmic sources at lower energies in the radio-wave to X-ray energy, is not available for γ -ray above 1 MeV [7]. The use of a low density converter-tracker, such as a gas detector, enables the measurement of the polarization fraction before multiple scattering ruins the azimuthal information carried by the pair [8].

γ -ray polarimetry would provide insight to understanding the value and turbulence of magnetic fields in the γ -ray emitting jets structure of most γ -ray emitting sources, and for example enable to decipher the leptonic and hadronic nature of the emitting particles in blazars [9].

*Corresponding author

Email addresses: yannick.geerebaert@polytechnique.fr
(Y. Geerebaert), philippe.gros@llr.in2p3.fr (Ph. Gros)

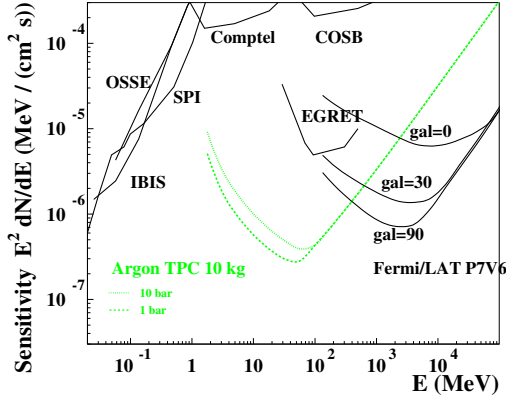


Figure 1: Differential sensitivity as a function of energy (argon-gas-based HARPO TPC, green) compared to the 90° galactic latitude performance of the Fermi-LAT [2] and of the Compton telescope COMPTEL [1]. Adapted from [6].

2. The HARPO detector

We have built a TPC which is using argon-based gas mixtures in the range 1–5 bar [10]. The drifted electrons are amplified by a hybrid amplifier whose performances have been characterized in detail [11].

We have exposed the detector to a tunable γ -ray source, using the head-on inverse Compton scattering of a laser beam on the 0.6 – 1.5 GeV electron beam of the NewSUBARU storage ring (Hyōgo, Japan) [12]. The detector was put so that the photon beam would be aligned with the drift direction z of the TPC, coming from the readout side, and exiting through the cathode.

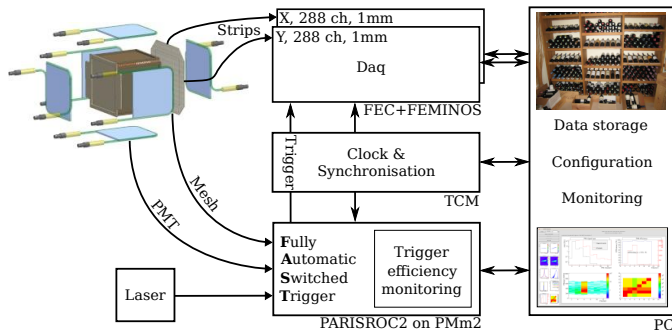


Figure 2: Global view of HARPO electronics.

The present detector is aimed at ground-validation tests, but we have designed it taking into account the constraint of space operation.

HARPO produces very fine 3D images of γ -conversions to e^+e^- pairs by tracking these events. This is done at a low cost in terms of power consumption and data flow in the presence of a large number of background noise tracks.

The TPC is a 30cm cubic field cage, enclosed with a copper cathode and a readout plane anode including a hybrid multi-stage amplification system composed of two GEM (Gas Elec-

tron Multiplier) + one MICROME GAS (128 μ m-gap bulk Micro MESH Gaseous Structure).

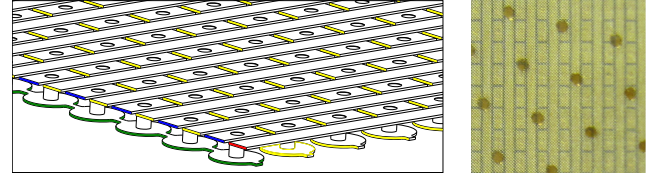


Figure 3: Left: Layout of readout plane of MICROME GAS. Only the copper of the PCB-based plane is shown. One x strip is coloured in red and one y pseudo-strip is in blue. y pseudo-strip are segmented in pads, connected together through via by an internal layer (green). Right: Top view of real PCB with pillars, keeping the mesh at a distance of 128 μ m of the readout plane.

As shown on figure 3, the signal is collected by two orthogonal series of strips (x & y), which, in our case, reduces the number of channels by a factor 144 compared to the equivalent pixel sensor. This reduction is only possible if the channel occupancy is low enough to avoid unsolvable ambiguities and comes at the cost of the need for off-line association of each x track to a track in the y view. Then, only 576 channels (x & y strips, 1 mm pitch) are read out and digitized at 33 MHz (up to 100 MHz) by eight AFTER chips mounted on two FEC boards. Channel data are then zero suppressed and sent to a PC via Gigabit Ethernet by two FEMINOS boards synchronized by one TCM board. These versatile boards were originally developed at IRFU for the T2K and MINOS experiments[13]. To mitigate the dead time induced by readout and digitization (1.6 ms) we developed a sophisticated trigger, with a multi-line system so as to provide real-time efficiency monitoring of each component.

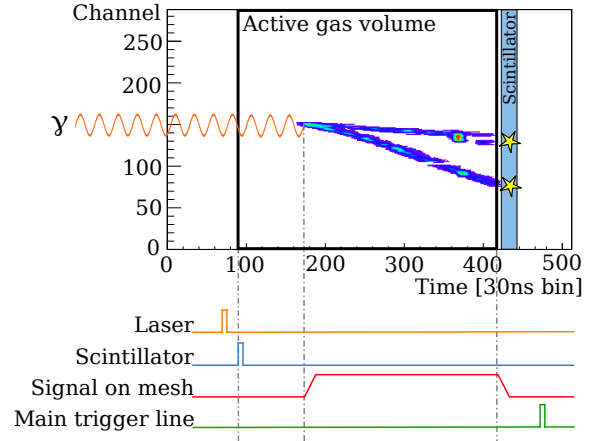


Figure 4: Typical timing of trigger in TPC.

To provide presence and timing informations on events, six scintillators, readout by PMT and PARISROC2 chip[14] mounted on a PMM2 board[15], surrounds the TPC.

The timing of the charge induced on the mesh is used for trigger. The signal, which is long and with unpredictable shape, corresponds to the time distribution of tracks in the TPC. To get a signal from the rising edge, we use a constant fraction

discriminator (CFD), which shows the beginning of the signal, and therefore the position of the beginning of the track. We can measure the delay between the start of the event and this signal to build a veto on tracks created upstream from the TPC. 125

The main line of the trigger select pair creation events which follows from the interaction of γ photon with nucleus of gas atom in the TPC. It is composed of: 130

- Veto on upstream scintillator (which reveal an interaction before the active gas region), 135
- signal on mesh of MICROMEAS with a veto based on presence of very early signal (we reject most of the γ -rays that convert in the material of the readout plane), 140
- signal in at least one of the five others scintillators,
- laser signal, whenever available (for pulsed laser), in coincidence with signal in scintillators.

This trigger suppressed the huge background rate from the accelerator (up to 5 kHz) by a rejection factor greater than two orders of magnitude [18] during the data taking campaign, where 60 millions of events, at 13 energy points, fully polarized and not polarized, have been recorded on disk. 145

3. Analysis of data from a polarised photon beam 110

We took data with HARPO TPC in a polarised photon beam at the NewSUBARU [12]. The photon is aligned with the drift direction z and arrives from the readout side. The detector was rotated around the z -axis to study the systematic angular effects related to the cubic geometry of the TPC. A total of about 60 million events were taken, with 13 different photon energies from 1.7 to 74 MeV, and 4 TPC orientations. Both polarised and unpolarised beams were used. 115

Figure 5 shows a pair conversion event as observed in the HARPO TPC. The two electron/positron tracks are visible in each of the two projection X-Z and Y-Z. 120

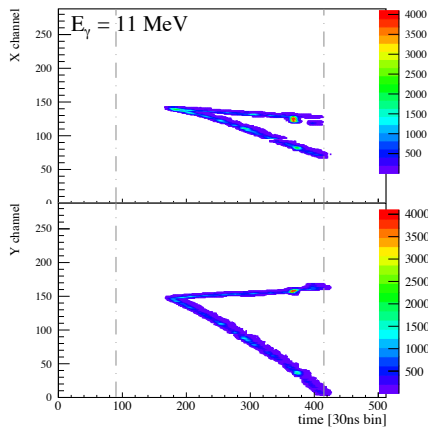


Figure 5: Example of a raw event in the HARPO TPC. The two tracks from the pair conversion of a 11 MeV photon are clearly visible.

The electron tracks were reconstructed on each projection using a closest neighbour search based on a Kalman filter [16]. Unfortunately, since the two tracks are difficult to disentangle near the vertex, it was impossible to use the Kalman filter to estimate the track direction near the vertex. The identified tracks were therefore fitted with a straight line. Then, the tracks reconstructed on each projection (X-Z and Y-Z) were paired together using their charge profile as a function of the drift time (equivalent to the Z coordinate). This way we can define tracks in 3D.

For each pair of reconstructed 3D track, point and distance of closest approach (POCA and DOCA) were calculated. We selected only the track pairs where the POCA was close enough to the vertex position, as estimated from the beam geometry. The azimuthal angle ω for a pair e^+e^- with direction \vec{u}^+ and \vec{u}^- is defined in Fig.1 of [17]. Using the fact that our photon beam is aligned with the z direction, ω is:

$$\omega = \arctan\left(\frac{u_z^- u_x^+ - u_z^+ u_x^-}{u_z^- u_y^+ - u_z^+ u_y^-}\right) \quad (1)$$

A distribution of ω is shown in Fig. 6 for several orientations of the detector with an unpolarised beam. The distribution is dominated by systematic fluctuations due to inefficiencies of the reconstruction algorithm in some track configurations and related to the cubic shape of the detector.

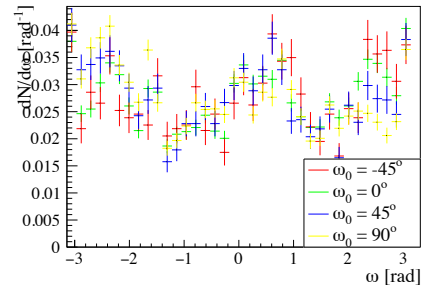


Figure 6: Azimuthal angle ω for one configuration of the TPC with 11 MeV photon beam. Only the statistical uncertainties are shown. Systematic effects dominate the distribution.

To compensate for these systematic effects, we took data with different orientations of the TPC with regard to the photon beam. By combining the data taken at different angles ω_0 of the TPC we obtain the distributions of $\omega - \omega_0$ shown on the upper two plots of Fig. 7. Most of the systematic fluctuations are averaged out, although a few remain. In these distributions we can already see a difference between the unpolarised (top) and polarised (middle) beam data. 145

Finally we divide the distribution for a polarised beam, by the unpolarised one. This way all the systematic effects cancel out, and only the polarisation asymmetry remains. Figure 7, bottom plot, shows this asymmetry. The measured polarisation angle $14.7^\circ \pm 6.5^\circ$ is consistent with the expected value of zero. The effective asymmetry, estimated at $6.25 \pm 1.42\%$, is significantly smaller than the theoretical value of 17% (see Fig.21 in [8]). 150

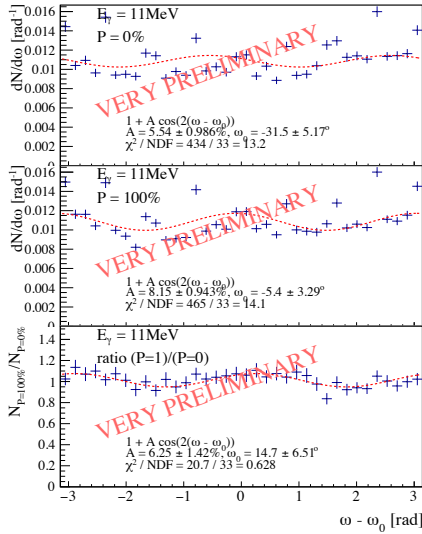


Figure 7: Distribution of the reconstructed azimuthal angle $\omega - \omega_0$ from pair conversions of 11 MeV photons in the TPC. Top: unpolarised photon beam. Middle: fully polarised photon beam. Bottom: ratio of the two distributions above. The systematic effects are cancelled, and an effective polarisation asymmetry of 6% is visible.

4. Discussion and outlook

The HARPO TPC was successfully used to measure pair conversions of photons from a few MeV to 74 MeV. The trigger using photomultipliers and the direct signal from the micromegas mesh performed a suppression of the background by nearly two orders of magnitude, with about 50% selection efficiency as shown in [18].

A first reconstruction algorithm has been applied to the data to extract the azimuthal angle of the electron-positron pair. By comparing data from polarised and unpolarised beam, we extract a first observation of the polarisation modulation for photons with energy 11 MeV and higher. The reconstruction efficiency is still very low, and many systematic effects remain to be understood. These results show that photon polarimetry in the pair production regime can be achieved with a TPC. A more appropriate reconstruction is being developed to increase the efficiency and the resolution.

These preliminary results demonstrate that the design of a space TPC is viable. A sophisticated hardware and software allows a reduction of the number of channels by several orders of magnitude. The next step will be the design of a balloon-borne TPC. It will be used to validate the trigger which is a key point for a successful space telescope. The trigger will have to extract approximately 10 Hz photon conversion signal from about 5000 Hz single-track background.

5. Acknowledgements

This work is funded by the French National Research Agency (ANR-13-BS05-0002).

References

- [1] V. Schoenfelder, Lessons learnt from COMPTEL for future telescopes, *New Astronomy Reviews* 48 (2004) 193–198. doi:doi:10.1016/j.newar.2003.11.027.
- [2] M. Ackermann, et al., The Fermi Large Area Telescope On Orbit: Event Classification, Instrument Response Functions, and Calibration, *Astrophys. J. Suppl.* 203 (2012) 4. doi:dx.doi.org/10.1088/0067-0049/203/1/4.
- [3] M. Tavani, V. Tatischeff, et al., The ASTROGAM gamma-ray space mission; A sensitive observatory for the MeV - GeV domain. In preparation.
- [4] Xin Wu, Meng Su, et al., PANGU: A High Resolution Gamma-ray Space Telescope, *Proc.SPIE Int.Soc.Opt.Eng.* 9144 (2014) 91440F. doi:dx.doi.org/10.1117/12.2057251.
- [5] A. Moiseev, et al., Compton-Pair Production Space Telescope (ComPair) for MeV Gamma-ray Astronomy, *ArXiv e-prints arXiv:1508.07349*.
- [6] D. Bernard, TPC in gamma-ray astronomy above pair-creation threshold, *Nucl. Instrum. Meth. A* 701 (2013) 225.
- [7] J. R. Mattox, Analysis of the COS B data for evidence of linear polarization of VELA pulsar gamma rays, *Astrophysical Journal* 363 (1990) 270–273. doi:dx.doi.org/10.1086/169338.
- [8] D. Bernard, Polarimetry of cosmic gamma-ray sources above e^+e^- pair creation threshold, *Nucl. Instrum. Meth. A* 729 (2013) 765. doi:dx.doi.org/10.1016/j.nima.2012.11.023.
- [9] H. Zhang, M. Böttcher, X-Ray and Gamma-Ray Polarization in Leptonic and Hadronic Jet Models of Blazars, *Astrophys. J.* 774 (2013) 18.
- [10] D. Bernard, HARPO - A gaseous TPC for high angular resolution γ -ray astronomy and polarimetry from the MeV to the TeV, *Nucl. Instrum. Meth. A* 718 (2013) 395–399. doi:dx.doi.org/10.1016/j.nima.2012.10.054.
- [11] P. Gros, et al., HARPO - TPC for High Energy Astrophysics and Polarimetry from the MeV to the GeV, *Proceedings of Science TIPP2014* (2014) 133.
- [12] S. Wang, et al., HARPO: a TPC concept for γ -ray polarimetry with high angular resolution in the MeV-GeV range, *J.Phys.Conf.Ser.* 650 (2015) 012016.
- [13] D. Calvet, A Versatile Readout System for Small to Medium Scale Gaseous and Silicon Detectors, *IEEE Trans. Nucl. Sci.* 61 (1) (2014) 675–682. doi:10.1109/TNS.2014.2299312.
- [14] S. Conforti Di Lorenzo, et al., PARISROC, an autonomous front-end ASIC for triggerless acquisition in next generation neutrino experiments, *Nucl. Instrum. Meth. A* 695 (2012) 373–378. doi:10.1016/j.nima.2011.11.028.
- [15] B. Genolini, et al., PMm2: Large photomultipliers and innovative electronics for the next-generation neutrino experiments, *Nucl. Instrum. Meth. A* 610 (2009) 249–252. arXiv:0811.2681, doi:10.1016/j.nima.2009.05.135.
- [16] R. Fruhwirth, Application of Kalman filtering to track and vertex fitting, *Nucl. Instrum. Meth. A* 262 (1987) 444–450. doi:10.1016/0168-9002(87)90887-4.
- [17] B. Wojtsekhowski, D. Tedeschi, B. Vlahovic, A pair polarimeter for linearly polarized high-energy photons, *Nuclear Instruments and Methods in Physics Research Section A: Accelerators, Spectrometers, Detectors and Associated Equipment* 515 (3) (2003) 605 – 613. doi:http://dx.doi.org/10.1016/j.nima.2003.07.009. URL <http://www.sciencedirect.com/science/article/pii/S0168900203023143>
- [18] S. Wang, étude d'une tpc, cible active pour la polarimétrie et l'astronomie gamma par création de paire dans harpo, Ph.D. thesis, École Polytechnique, in *Frrench* (9 2015).